# Pool boiling of Novec-649 on minichannels filled with copper foam

*Robert* Pastuszko[1*], *Norbert* Dadas[1], and *Robert* Kaniowski[1]

[1]Kielce University of Technology, Faculty of Mechatronics and Mechanical Engineering, al. 1000-lecia Państwa Polskiego 7, PL-25-314 Kielce, Poland

**Abstract.** The article describes the experimental investigation of pool boiling heat transfer on minichannels with filling in the form of porous structure (copper foam). The results were compared with the data for a smooth surface and the minichannels without additional fillings. Tests were carried out for the boiling liquid Novec-649. Surfaces partially filled with porous structure were formed by inserting pieces of copper foam into the minichannels of 5 mm in depth and 1 mm width. Minichannels completely filled with copper foam formed the surface of MCC-F. The measurements were made with an increase in heat flux. The heat transfer coefficient obtained was four times higher than for the smooth surface. Additional foam fillings increased the heat transfer coefficient and reduced superheat for heat fluxes less than 100 kW/m$^2$. Visualisation was made using a high-speed camera which allowed to determine the diameters of the growing bubble.

## 1 Introduction

New surfaces that increase heat transfer rate (enhanced surfaces) are being extensively studied in many research centres in the United States, Europe, China, Japan, Iran, Brazil and South Korea.

Examples of surfaces with mini/micro channels and a porous structure in the form of metal foam, tested in the last 10 years, are presented in Table 1.

**Table 1.** Types of structures with micro, minichannels and metal foams for pool boiling enhanced heat transfer

| Type | Reference | Configuration | Liquid | The highest HTC |
|---|---|---|---|---|
| Open micro/minichannels | Cooke and Kandlikar [1] | silicon microchannels 40 – 200 μm wide and 180 – 275 μm deep, etched in silicon plates | water | 73 kW/m$^2$K |
| | Kalani and Kandlikar [2] | copper microchannels 245 – 470 μm deep and 194 – 406 μm wide | ethanol | 72 kW/m$^2$K |
| | Gheitaghy et al. [3] | copper surface on 45º inclined microchannels (widths: 0.5—0.7 mm, depths: 0.5—1 mm) | water | about 120 kW/m$^2$K |
| | Kaniowski et al. [4] | microchannels 0.2-0.4 mm deep, 0.3 mm wide (HTC referred to the area of the heating cylinder - the tested area is 2 times smaller) | water Novec | 64 kW/m$^2$K (water) and 8 kW/m$^2$K (Novec-649) |
| | Kaniowski and Pastuszko [5] | copper microchannels 0.3 mm wide, 0.2—0.5 mm deep (note as above) | water ethanol | 63 kW/m$^2$K (water), 20 kW/m$^2$K (ethanol) |
| Plain metal foams/ | Manetti et al. [6] | copper foams, porosity 0.9, thickness 1—3 mm | HFE-7100 | about 20 kW/m$^2$K |
| | Zhu et al. [7] | copper foams, 10 and 20 ppi, porosity 90—98%, thickness 5 mm | R113 | up to 4.7 kW/m$^2$K |
| | Yang et al. [8] | Cu foam 30-90 ppi, porosity 0.88-0.95, thickness 1—5 mm | water | up to 150 kW/m$^2$K |
| Gradient metal foams | Huang et al.[9] | 40 ppi nickel foam, 10 ppi copper foam, thickness 4 mm, porosity 0.98 | water | about 35 kW/m$^2$K |
| | Xu and Zhao [10] | copper and nickel foams, pore densities from 5 to 100 ppi, porosity of 0.98 | water | up to 240 kW/m$^2$K |
| | Pratik et al. [11] | foam-like hierarchical hexagonal boron nitride (h-BN) nanomaterial | water | up to 37 kW/m$^2$K |
| | Xu et al. [12] | grooved array copper foam surfaces, porosity 0.9–0.98, 5–40 ppi, thickness 5–7 mm. | water | up to 90 kW/m$^2$K |
| | Qu et al [13] | copper V-shaped grooves, porosity of 0.95, 100-130 ppi, thickness 2 and 4 mm | water | about 93 kW/m$^2$K |
| | Xu and Zhao [14] | trapezoid-shaped copper-foam fins, pore densities 100–130 ppi, porosity 0.95, thickness 2—6 mm | water | about 90 kW/m$^2$K |

* Corresponding author: tmprp@tu.kielce.pl

## 2 Experimental setup

The experimental setup to determine the heat transfer coefficient and diameter of the bubbles was presented in Fig. 1a. The heat supplied by the resistance heater to the main module can be adjusted using an autotransformer, and the power can be read on a wattmeter. The sealed sample formed the basis of a vessel with four rectangular glass walls, which made it possible observing bubble formation and growth. Photographs at 1000 fps were taken with a high-speed camera.

To improve the quality of the images, the main module was lighted with a SCHOTT KL 2500 LED. The linearity of the heat flux supplied by the heater to the specimen through the copper cylinder (Fig. 1b) was determined using four K-type thermocouples ($T_5$ – $T_8$) placed in the heating cylinder. Two additional thermocouples $T_3$ and $T_4$ (Fig. 1b,c) were placed directly below the sample. The specimen was soldered to the copper bar using a thin layer of tin. Differences in temperature indicated by the thermocouples $T_3$ and $T_4$, placed between the specimen and the cylinder, were less than 0.2 K. The main module worked as a thermosiphon – the condensed vapour returned to the vessel with the boiling liquid. Two thermocouples ($T_1$, $T_2$) were placed in the liquid above the specimen; they allowed us to determine the changes in temperature of the liquid during boiling.

The experiments were carried out at atmospheric pressure. The temperature difference between the thermocouples $T_1$ and $T_2$ was slightly greater than the measurement error, not exceeding 0.4 K.

The measurement uncertainties according to [15] were determined as follows:

- relative uncertainties in determining the heat transfer coefficient were about 24% – 3% for HTC in the range 8 – 24 kW/m$^2$K
- relative uncertainties in determining the heat flux varied between 22% to 4% for heat flux in the range 20 – 240 kW/m$^2$

Depending on the filling configuration, there were different lengths of the foam sections in the channels, as well as spaces between them. Figure 1c shows an arrangement of the porous fillings for different specimens, described in Table 2. The MC samples did not have porous fillings inside the minichannels, while the MCC-F specimen had a fully filled channel with porous structures. Foam with a porosity of 98% and pore densities of 100 ppi was used for the experiments.

**Table 2.** Specimen code and specification.

| Code | $p_p$, mm | $\delta_p$, mm | $n_p$ | $l_p$, mm |
|---|---|---|---|---|
| MC | - | - | - | - |
| MCC-F | - | 1 | 1 | 27 |
| MCC-F-3.6-0.3-3 | 3.6 | 0.3 | 3 | 1.5 |
| MCC-F-4.2-0.5-2 | 4.2 | 0.5 | 2 | 2 |

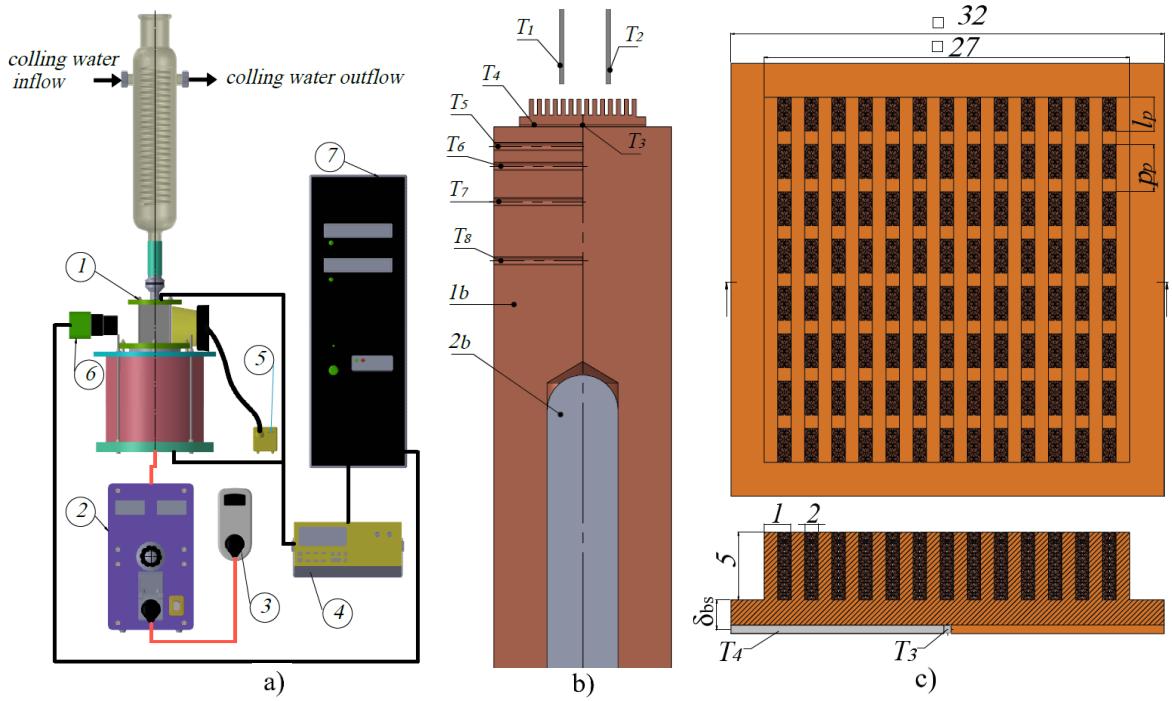


**Fig. 1.** a) Experimental setup, 1 – main module, 3 – autotransformer, 3 – wattmeter, 4 – data logger, 5 – light, 6 – high speed camera, 7 – PC, b) Arrangement of thermocouples, 1b – heating cylinder, 2b – cartridge heater, c) Specimen filled with porous foam structure.

## 3 Results

Figure 2 shows that at low heat fluxes the heat transfer coefficient (HTC) was higher when porous fillings were used. With an increase in the heat flux, a tendency toward a sharp decrease in HTC was observed along with a larger amount of foam filling the space in the channel. The minichannels with foam filling had higher superheating depending on the amount of filling (Fig. 3). Despite this, the heat transfer coefficient was several times higher than that of a plain smooth surface. MCC-F had one and a half times higher HTC than MC for a heat flux of about 50 kW/m². The superheat at the heat flux of about 50 kW/m² was lower for the MC by one and a half times than for the MCC-F. In the heat flux range 110 – 120 kW/m², the foam-filled specimens began to decrease the HTC compared to the minichannles without porous structure (MC). The highest difference in HTC for heat flux exceeding 120 kW/m² was observed for the MCC-F specimen, and the smallest was for the sample with longer distances between channel fillings (MCC-F-4.2-0.5-2). The highest HTC was reached for the MC specimen, the value was 25.4 kW/m²K for the heat flux 382.5 kW/m². The performance at high heat flux for specimen without porous fillings was 20% better compared to MCC-F-4.2-0.5-2.

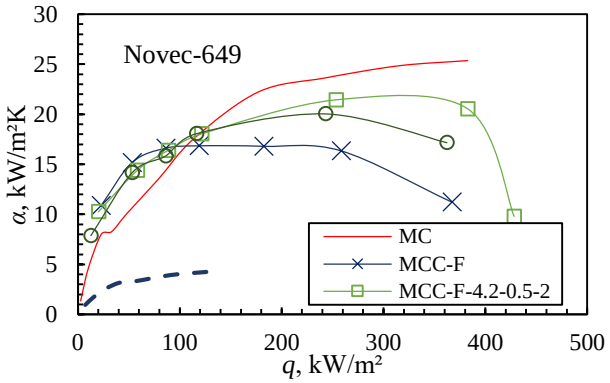


**Fig. 2**. Boiling curves for Novec-649, heat transfer coefficient versus heat flux.

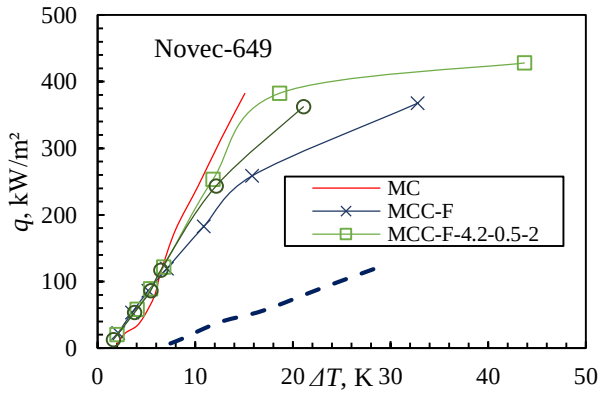


**Fig. 3.** Boiling curves for Novec-649, heat flux versus superheat.

The attempts to predict the diameter of the bubbles that grow during pool boiling were discussed in [16]. The authors mentioned the equation (1) for bubble growth in uniformly superheated liquid:

$$D = \phi_c \frac{4Ja\sqrt{a\tau}}{\sqrt{\pi}} \quad (1)$$

where $\tau$ is the time, $a$ is the liquid thermal diffusivity and $\phi_c$ is sphericity correction factor, $\phi_c = \sqrt{3}$ according Plesset and Zwick. The Jakob number can be calculated from the equation:

$$Ja = \frac{\rho_l c_{pl} \Delta T}{\rho_v i_{lv}} \quad (2)$$

Liquid thermal diffusivity is described by the equation:

$$a = \frac{\lambda_l}{c_{pl}\rho_l} \quad (3)$$

Equation (1) was related to a plain surface. To correlate this equation for an extended surface with additional pieces of copper foam inside minichannels, the authors suggest the use of correction factor $C_{mc}$= 4.85, thus:

$$D_{mc} = C_{mc}\phi_c \frac{4Ja\sqrt{a\pi\tau}}{\pi} \quad (4)$$

The calculations according Eqs (1) and (4) were presented in Fig. 4 compared to the experimental data achieved during pool boiling visualization. The accuracy of bubble diameter measuring of 0.2 mm was assumed. The parameters of Novec-649 required for the calculations are shown in Table 3.

**Table 3.** Parameters of saturated Novec-649

| $T_{sat}$ °C | $\rho_l$ kg/m³ | $\rho_v$ kg/m³ | $c_{pl}$ J/kgK | $i_{lv}$ kJ/kg | $\lambda_l$ W/mK | $\sigma_l$ N/m |
|---|---|---|---|---|---|---|
| 49 | 1532 | 13.4 | 1118 | 88 | 0.054 | 0.0092 |

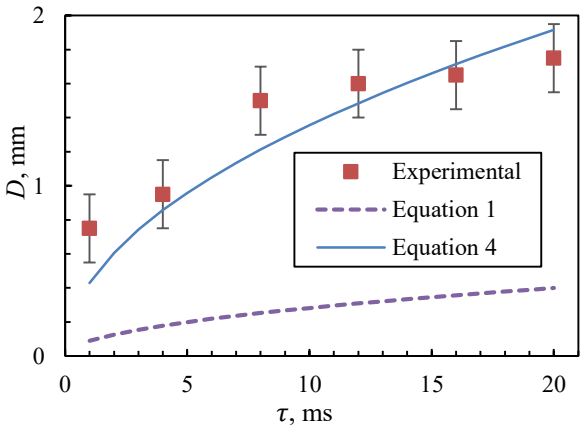


**Fig. 4**. Diameter of the growing bubble versus time.

## 4 Visualization of boiling

The bubbles formed at the minichannels outlets are shown in Fig. 5. By observing the places of growth of the bubbles and determining their diameters during growth, it is possible to better understand the mechanics that appear during the experiments. Bubbles were formed in the spaces between the porous structures and the liquid that was sucked by the porous fillings.

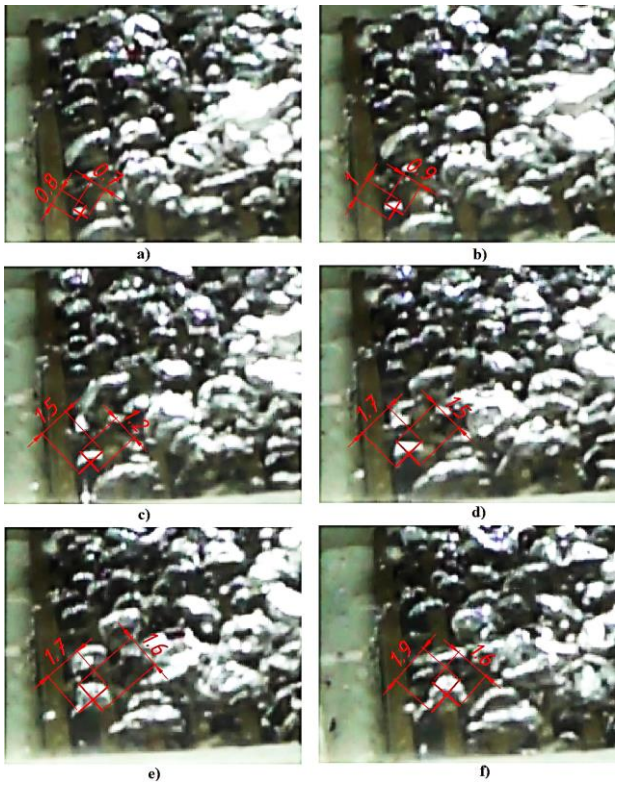


**Fig. 5.** Visualization of the pool boiling of Novec-649 on the surface of the minichannels surface MCC-M-4.2-0.5-2, $q$ = 27.9 kW/m$^2$, a) t = 1 ms, b) t = 4 ms , c) t = 8 ms, d) t = 12 ms, e) t = 16 ms, f) t = 20 ms.

## 5 Conclusions

Based on the data presented in this paper, the following conclusions were drawn:

- For the Novec-649 working fluid, the highest heat transfer coefficients at heat fluxes less than 120 kW/m$^2$ were obtained using minichannels with additional porous filling. At larger heat fluxes, the largest HTC provided minichannels without fillings.
- The proposed surfaces with partially filled minichannels with porous structure are a new concept among structures designed to intensify the pool boiling heat transfer.
- The experiments carried out show that under certain conditions, fillings in the form of copper foam can improve the critical heat flux.
- The spaces between the porous fillings allowed for the efficient releasing of the vapour, and a significant enhancement was achieved both in CHF and in HTC.
- The proposed modified Plesset-Zwick relationship enables the presentation of changes in the diameter of the growing bubble as a function of time with satisfactory accuracy.

## Nomenclature

$a$ – liquid thermal diffusivity $[m^2/s]$,
$c_p$ – specific heat at constant pressure $[J/kgK]$,
$C$ – correction factor
$D$ – diameter of the bubble $[mm]$,
$i_{lv}$ – heat of vaporization $[kJ/kg]$,
$Ja$ – Jakob number $[-]$,
$l$ – length [mm],
$p$ – pitch [mm]

**Greek symbols**

$\Delta T$ – superheat for specimen surface $[K]$,
$\delta$ – thickness [mm],
$\lambda$ – thermal conductivity $[W/mK]$,
$\rho$ – density $[kg/m^3]$,
$\sigma$ – surface tension [N/m],
$\tau$ – time $[s]$,
$\phi_c$ – sphericity correction factor,

**Subscripts**

$l$ – liquid phase,
$mc$ – minichannels,
$p$ – pore, porous,
$v$ – vapour phase.

## References

1. D. Cooke, S.G. Kandlikar, J. Heat Transfer, **133** (2011),
2. A. Kalani, S.G. Kandlikar, proc. ASME 10th Int. Conf. Nanochannels, Microchannels, and Minichannels **10** (2012),
3. A.M. Gheitaghy,. A. Samimi, H. Saffari, Appl. Therm. Eng. **126** (2017),
4. R. Kaniowski, R. Pastuszko, Ł. Nowakowski, EPJ Web Conf. **143** (2017),
5. R. Kaniowski, R. Pastuszko, EPJ Web Conf. **180** (2018),
6. L.L. Manetti, A.S.O.H. Moita, Int. J. Heat Mass Transf. **152** (2020),
7. Y. Zhu, H. Hu, G. Ding, H. Peng, X. Huang, D. Zhuang, J. Yu, Int. J. Refrigeration **34** (2011),
8. Y. Yang, X. Ji, J. Xu, Int. J. Therm. Sci. **49** (2010),
9. R.L. Huang, C.Y. Zhao, Z.G. Xu, Int. J. Multiph. Flow **103** (2018),
10. Z.G. Xu, C.Y. Zhao, Int. J. Heat Mass Transf., **85** (2015),
11. K.C. Pratik, A. Nammari, T. S. Ashton, A. L. Moore, Int. J. Heat Mass Transf. **95** (2016),
12. Z.G. Xu, Z.G. Qu, C.Y. Zhao, W.Q. Tao, Int. J. Heat Mass Transf. **77** (2014),
13. Z.G. Qu, Z.G. Xu, C.Y. Zhao, W.Q., Int. J. Multiph. Flow **41** (2012),
14. Z.G. Xu, C.Y. Zhao, Appl. Therm. Eng. **60** (2013)
15. R. Pastuszko, R. Kaniowski, N. Dadas, M. Bedla-Pawlusek, Int. J. Heat Mass Transf. **179** 2021
16. R. Cole, H.L. Shulman, Int. J. Heat Mass Transf. **9** (1966).